



RESEARCH LETTER

10.1029/2022GL101078

Remarkable Changes in the Dominant Modes of North Pacific Sea Surface Temperature

Benjamin E. Werb¹ and Daniel L. Rudnick¹ ¹Scripps Institution of Oceanography, La Jolla, CA, USA

Key Points:

- The calculation of empirical orthogonal functions and principal components of North Pacific sea surface temperature is revisited
- The period of persistent marine heatwaves since 2014 has caused most energetic modes to change
- A conclusion is that indices based on empirical orthogonal function analysis may not be as useful as climate continues to change

Supporting Information:

Supporting Information may be found in the online version of this article.

Correspondence to:

D. L. Rudnick,
drudnick@ucsd.edu

Citation:

Werb, B. E., & Rudnick, D. L. (2023). Remarkable changes in the dominant modes of north Pacific sea surface temperature. *Geophysical Research Letters*, 50, e2022GL101078. <https://doi.org/10.1029/2022GL101078>

Received 30 AUG 2022

Accepted 1 FEB 2023

Author Contributions:

Conceptualization: Daniel L. Rudnick
Formal analysis: Benjamin E. Werb, Daniel L. Rudnick
Funding acquisition: Daniel L. Rudnick
Investigation: Benjamin E. Werb, Daniel L. Rudnick
Methodology: Benjamin E. Werb, Daniel L. Rudnick
Project Administration: Daniel L. Rudnick
Resources: Daniel L. Rudnick
Software: Benjamin E. Werb, Daniel L. Rudnick
Supervision: Daniel L. Rudnick
Visualization: Benjamin E. Werb
Writing – original draft: Benjamin E. Werb, Daniel L. Rudnick

© 2023. The Authors.

This is an open access article under the terms of the [Creative Commons Attribution License](https://creativecommons.org/licenses/by/4.0/), which permits use, distribution and reproduction in any medium, provided the original work is properly cited.

Abstract The analysis revisits the calculation of the empirical orthogonal functions (EOFs) and principal components (PCs) of sea surface temperature (SST) in the North Pacific from 1950 to 2021. The first EOF and PC of SST has proven to be such a useful metric of variability in the North Pacific that it is called the Pacific Decadal Oscillation (PDO). We find that the period of persistent marine heatwaves beginning in 2014 caused a fundamental change to the first EOF and PC of SST (calculated using data from 1950 to 2021) as compared to the established PDO spatial pattern (calculated using data from 1950 to 1993). The second EOF of SST has also changed during this period, both in spatial pattern and in the amount of variance explained. A conclusion is that the PDO and other EOF based metrics may not be as useful in the future as climate continues to change.

Plain Language Summary The Pacific Decadal Oscillation (PDO) is a widely used measure of the temperature variability in the North Pacific Ocean. The PDO is the result of a well-known technique called empirical orthogonal function (EOF) analysis that isolates the most energetic modes of variability of the analyzed variable. The first time EOF analysis was applied to oceanographic data was in the 1970's when it was used to identify the most energetic modes of North Pacific sea surface temperature (SST). The first EOF of North Pacific SST has proved so useful as a measure that it received the moniker PDO. Our analysis suggests that a period of persistent marine heatwaves in the North Pacific since 2014 has been so powerful that this first mode of variability of SST has fundamentally changed and the PDO may not be as useful an indicator as it once was.

1. Introduction

Sea surface temperature (SST) in the North Pacific has long been known to play a fundamental role in climate variability. Beginning in the 1960s, Jerome Namias noted that patterns of SST anomalies influenced atmospheric variability on large scales (Namias & Cayan, 1981). To identify these patterns, the first empirical orthogonal function (EOF) analyses of North Pacific SST were performed (Davis, 1976; Weare et al., 1976). An EOF analysis in its simplest form takes a variable like SST that is a function of space and time and expresses it as a sum of products of spatial and temporal modes. The spatial modes are typically called EOFs, and the temporal modes are called amplitudes or principal components (PCs). The first EOF and PC proved such a useful measure of large-scale, low-frequency variability in the North Pacific that it was given the name Pacific Decadal Oscillation (PDO) by Mantua et al. (1997). The PDO has proved to be a valuable measure of basin-scale variability in the North Pacific that continues to be used in fisheries (Weber et al., 2021). A number of studies have addressed changes in the PDO temporal index (Bond et al., 2003; Litzow, Hunsicker, et al., 2020; Litzow, Malick, et al., 2020). The PDO has also been widely used as a metric of climate variability in the North Pacific with effects on atmospheric processes, although, as noted by Newman et al. (2016), this could also be related to the El Niño Southern Oscillation (ENSO).

Since 2014, the eastern North Pacific has experienced a series of marine heatwaves (Bond et al., 2015) with pronounced effects on the California Current System (Zaba & Rudnick, 2016). We address the question of how this period of anomalous warmth in the eastern North Pacific is reflected in the EOFs of North Pacific SST. To ensure that recent warming contributes to the variability we do not remove a trend before applying the EOF analysis. Retaining the trend is consistent with the original EOF analysis of the North Pacific (Davis, 1976) and more recently by Johnstone and Mantua (2014) who calculated the EOFs of SST east of the dateline. Notably, Johnstone and Mantua (2014) define a Northeast Pacific (NEP) index by averaging over the positive region of their first EOF in the eastern Pacific. At issue is whether the EOFs describe variability relative to the trend, or whether they are influenced by warming at the end of the record. By calculating EOFs and PCs over records of increasing length, we demonstrate that this period of persistent marine heatwaves (MHWs) has transformed the

Writing – review & editing: Benjamin E. Werb, Daniel L. Rudnick

spatial pattern of the first EOF of North Pacific SST to such an extent that the PDO may no longer be as serviceable a metric of SST variability as currently regarded.

2. Data

We use monthly mean SST for the period 1950–2021 in the region 120°E–110°W, 20°N–60°N, from the NOAA Extended Reconstructed Sea Surface Temperature V5 data product (ERSSTv5) with 2° resolution in longitude and latitude and confirm our results with the HadISST data product (see Supporting Information S1). ERSSTv5 consists of in situ measurements collected from ships, buoys, and Argo floats, excluding remotely sensed satellite data, and uses a series of reconstruction techniques to extend global records back to 1854 (Huang et al., 2017b). Spatial coverage is the foundation of a strong EOF/PC analysis (Huang et al., 2017b) so this study uses only the data from the modern era, following previous studies (Newman et al., 2003). ERSSTv5 and HadISST are both data products derived from observations and there are systematic SST differences between the two products in the central and north-eastern Pacific causing large discrepancies in the resulting PDO indices (Wen et al., 2014). We use the ERSSTv5 product, following the NOAA PDO calculation.

3. Analysis

The objective of this analysis is to revisit the calculation of EOFs and PCs as first done by Davis (1976). The first step is to remove the seasonal cycle from ERSSTv5 by computing the average monthly temperature and subtracting it from each respective month. The result of this procedure is a data set of SST anomalies (SSTa) relative to the annual cycle. The global warming trend was not removed from the time series so that the trend contributes to the variance described by the EOFs; previously Johnstone and Mantua (2014) also did not remove a trend for the same reason. We apply an EOF analysis to find the most energetic modes of variance. The resulting EOFs and PCs are orthogonal to one another and are ordered by the variance explained. The first five EOFs account for over 50% of the total variance, the detailed distribution between the EOFs is covered below. To calculate the EOFs and PCs, we use a singular value decomposition of the anomaly data set.

The PDO spatial pattern and Index were recreated with SSTa from ERSSTv5 by doing the EOF analysis only for data during 1950–1993. The EOF from this analysis is then projected onto the full time series to create the PDO Index and normalized to have unit length in the L2 norm.

The EOF analysis was done on successively longer time series starting with 1950–1970 and increasing yearly to 1950–2021. The results of this analysis are shown in several ways including EOF/PC pairs and by variance explained. Percent variance is calculated by squaring the singular values and dividing by the trace of the matrix squared. As a measure of structure, we calculate the percentage of the grid points where the EOFs are greater than zero and find that the structure of the EOFs changes over time. See Figure S4 in Supporting Information S1 for a bootstrap calculation assessing significance.

4. Results

The spatial pattern of the PDO for this paper is calculated as the first EOF of SST from 1950 to 1993, exclusively removing the annual cycle, and the projection onto this spatial pattern produces the PDO index (Figure 1). This is distinct from the original calculation which is done on data detrended using the anomaly deviation method (Mantua et al., 1997; Zhang et al., 1997). The correlation coefficient between our version of the PDO and the original PDO is 0.97. That the correlation is so high suggests that our data and procedure are close enough to those used originally, and that whether a trend is removed from the data has little effect on the result. The important point here is that the PDO spatial pattern is fixed in 1993 while the PDO Index evolves.

The first EOF of SST is calculated in blocks starting with the period 1950–1970 and increasing by 10-year increments to a maximum of 1950–2021 (Figure 2). The spatial pattern of the first EOF is relatively consistent for successively longer time periods up to 1950–2010 (Figures 2a–2e). The addition of the last decade to the calculation results in a significant change in the EOF, with a larger positive region in the eastern Pacific and a smaller negative lobe in the central Pacific. This change is due to persistent and strongly positive SST anomalies in the eastern and interior/western North Pacific. At its peak, the first MHW in this period (popularly referred to as “The Blob”; Bond et al., 2015) reached a temperature anomaly of +2.5°C, and impacted

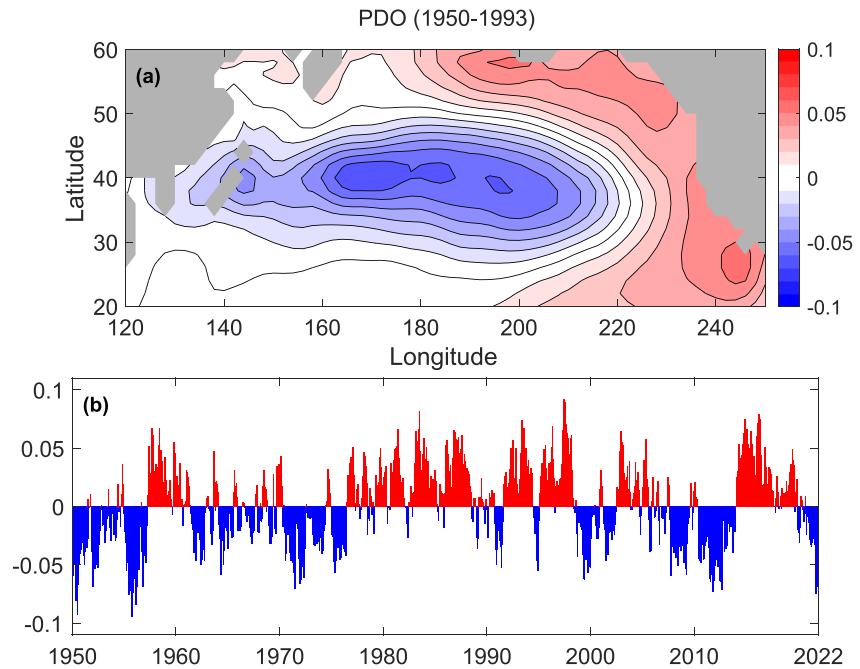


Figure 1. (a) PDO spatial pattern calculated as the first EOF of SST from 1950 to 1993. (b) The PDO Index formed by the projection of the PDO spatial pattern onto the full time series of SST anomalies from 1950 to 2021.

both marine ecosystems and weather patterns. This was followed by the 2014–2016 El Niño (L’Heureux et al., 2017; Rudnick et al., 2017), and the 2019 MHW (Amaya et al., 2020), resulting in continued warm anomalies in the eastern North Pacific. This anomalous warmth has largely remained in the California Current System (Ren & Rudnick, 2021), resulting in a fundamental change to the leading EOF of SST in the North Pacific.

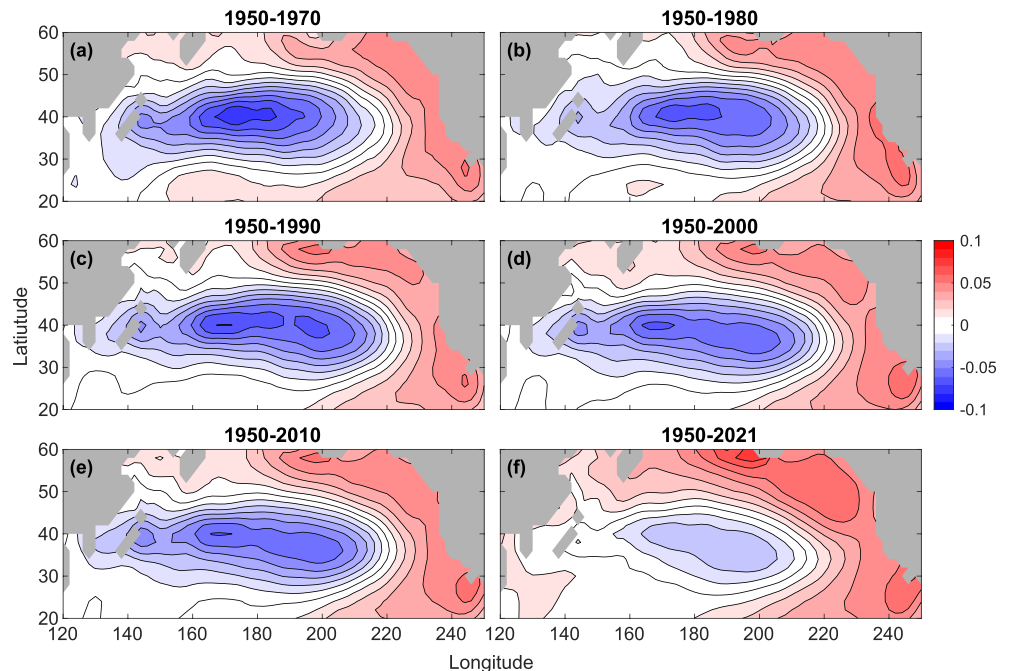


Figure 2. The first EOF of SST over the PDO region (120°E–110°W, 20°N–60°N). Panels (a–f) show the same spatial pattern calculation with a changing time series highlighting the effects of ocean warming in the last decade.

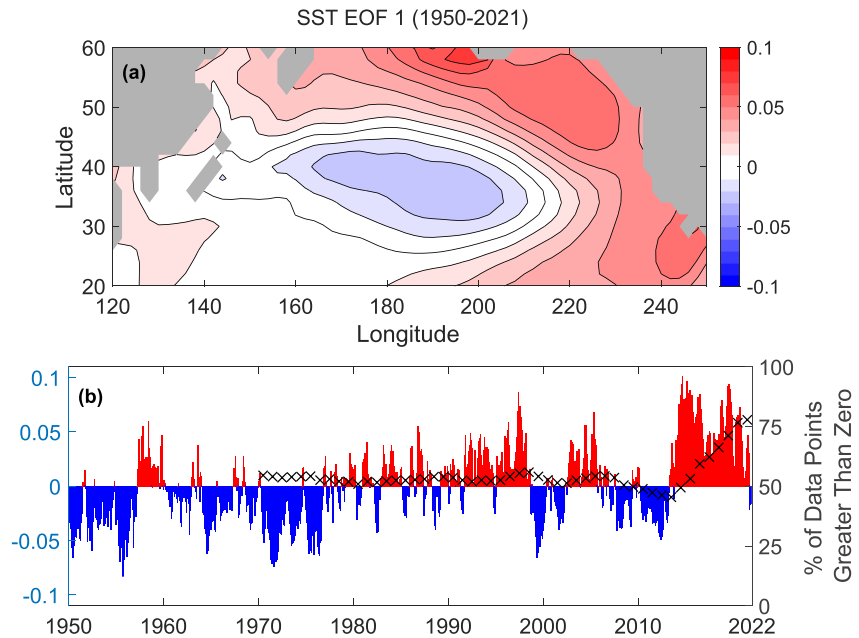


Figure 3. (a) The first EOF of SST over the PDO region for the entire time series (1950–2021). (b) The principal component for the first EOF is shown on the left y-axis, with red bars indicating positive years and blue bars indicating negative years. The right y-axis (x symbols) shows the percentage of grid points greater than zero in the first EOF from 1970 to 2021.

The first PC for the period 1950–2021 is dominated by an era of frequent MHW's from 2014 to 2021 (Figure 3). The combination of this strong warming phase at the end of the record and the cold phase at the beginning in this PC reflects a warming trend during 1950–2021 in the eastern Pacific. The inclusion of the trend in the time series allows it to be represented in the first PC and shows that a great deal of the warming is in recent years. This PC (Figure 3b) should be compared to the PDO Index (Figure 1b), especially regarding the recent warming. The PDO Index became negative in 2019 due to the impacts of persistently positive SSTa in the interior north Pacific on the negative lobe of its spatial pattern, while the first PC of the complete record remained positive until very late in 2021. That is, the first PC of the full time series fairly reflected the recent warming in the eastern Pacific while the PDO Index did not.

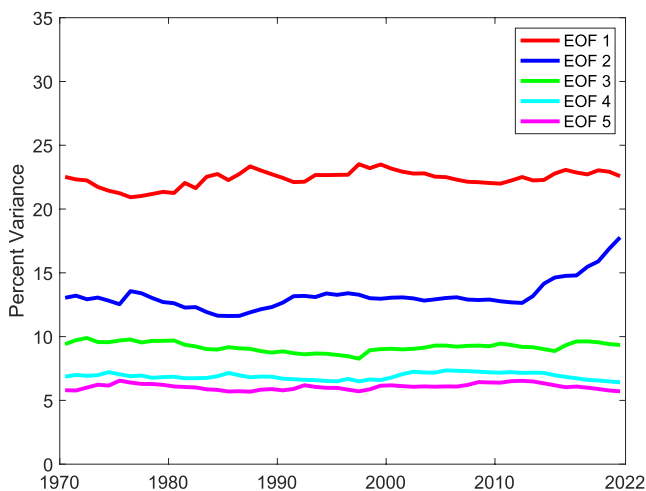


Figure 4. The percent variance accounted for by each EOF of the SST data set over the period of 1970–2021.

A measure of the spatial shape of the first EOF is the number of positive values in the 2° by 2° spatial grid. The first EOF is calculated over successively longer time periods, increasing by 1 year each, and the percentage of positive values is plotted in Figure 3b. The size of the positive region in the eastern Pacific stays relatively constant with roughly half the points greater than zero until 2014, after which the positive region rapidly increases in size to cover 77% of the North Pacific in 2021. The results are similar for HadISST data, with the positive region covering 65% of the Pacific (Figure S1.3 in Supporting Information S1). Such a fast rate of change in the shape of the first EOF is unprecedented, with roughly one-quarter of the North Pacific's area between 20° and 60°N changing polarity in the EOF. The relative consistency in the spatial pattern before 2014 is strong support for the usefulness of the PDO during the period 1950–2014 while the changes since 2014 suggest that the PDO is no longer the best descriptor of variance in SST in the North Pacific.

The percent variance explained by each of the first five EOFs is calculated from successively longer time periods (Figure 4). Throughout the record, EOF 1 has explained approximately 23% of the variance in SST. EOF 2 accounted for approximately 13% of the variance in SST until 2014, after which it increased to nearly 18%. This increase occurred simultaneously with

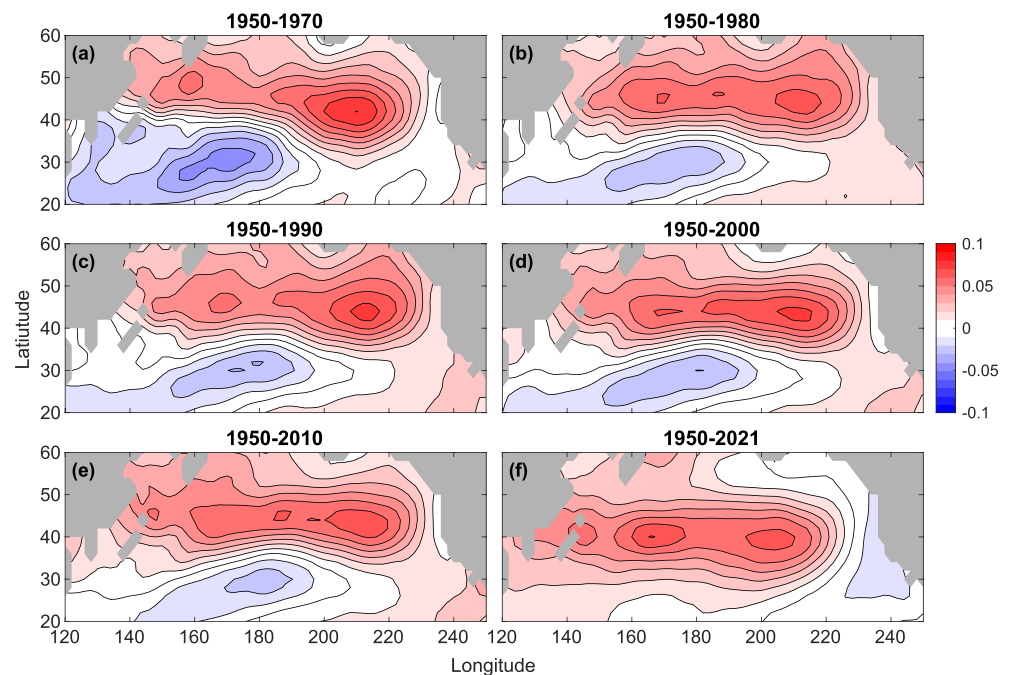


Figure 5. The second EOF of SST over the PDO region (120°E–110°W 20°N–60°N). Panels (a–f) show the same spatial pattern calculation with a changing time series.

the changing spatial pattern of EOF 1 in response to the MHW's. Interestingly the MHW's have changed patterns in such a fundamental way that the second EOF has risen in importance for describing SST variability in the North Pacific.

At the start of the time series the second EOF of SST was composed of two distinct lobes: positive in the north and negative in the south (Figure 5). Like EOF 1, this pattern remains consistent through 2010 (a–e), and then undergoes a change of shape after adding the most recent decade to the record (f). The positive lobe has recently filled up nearly all the North Pacific (Figure 5f). With the growth of this positive lobe, a small negative lobe has grown in the eastern North Pacific. In a sense, there has been a reshuffling of the regions affected by EOFs 1 and 2 (comparing Figures 2 and 5) in response to the period of persistent MHW's from 2014 to 2021. There is no longer a single EOF/PC pair that describes variance in the 30–50°N latitude band where the first two EOFs are both large.

The second PC is mostly positive from 1990 to 2021 and strongly positive from 2014 to 2021 (Figure 6b), reflecting the positive SSTa across much of the North Pacific that EOF 1 alone does not capture. The weak negative lobe in the second EOF lessens the warming near the coast of North America. As EOF 2 describes less of the variance than EOF 1, it might be expected that its shape is more variable when calculated over different time periods, interestingly, the positive lobe in EOF 2 has grown steadily when calculated over successively longer time periods (Figure 6b, x-ticks). The positive lobe of EOF 2 filled up 98% of the North Pacific when calculated over the period 1950–2018 and similarly for HadISST data at 93% (Figure S1.6 in Supporting Information S1). While EOF 2 has not been invoked as often as the PDO as a measure of SST variability, the robust evolution since 2014 is still worthy of note.

5. Conclusions

The fundamental result of this study is that the first EOF of SST in the North Pacific has changed starting in 2014. For more than 20 years, the PDO has been used to describe the state of the North Pacific. However, since the marine heatwave of 2014, there have been remarkable changes to the dominant mode of SST in the North Pacific. The spatial pattern of the first EOF of SST from 1950 to 2021 is notably different from the PDO, suggesting that though the PDO served as a useful metric of SST variations until 2014 (Johnstone & Mantua, 2014), it may

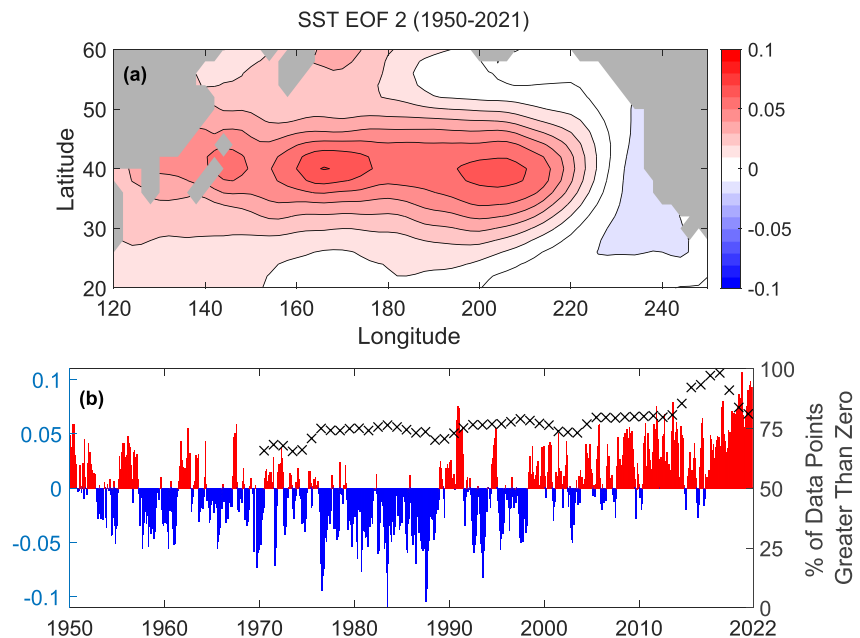


Figure 6. (a) The second EOF of SST over the PDO region for the entire time series (1950–2021). (b) The principal component for the second EOF is shown on the left y-axis using colored bars. The right y-axis (x symbols) shows the percentage of data points greater than zero in the second EOF from 1970 to 2021.

no longer be as effective a climate index for the North Pacific. From 1950 until the 2014 MHW, the first EOF remained consistent in its proportion of positive and negative regions with both taking up roughly half the area of the North Pacific (and with the positive region taken to be the eastern Pacific). When EOFs are calculated from 1950 to endpoints after 2014, the first EOF has a maximum positive region covering 77% of the North Pacific, with a PC indicating the largest anomalies on record. These changes to the first EOF/PC of North Pacific SST are nothing short of remarkable.

In concert with these changes, the second EOF/PC of SST has also undergone profound evolution since 2014. This second EOF now accounts for approximately 18% of the variability, growing from 13% during the 1950–2013 period. The spatial structure of the second EOF now is positive over almost the entire basin, with a PC that has grown strongly positive in the last several years. Thus, the second EOF/PC describes warming over much of the Pacific not in the positive lobe of the first EOF.

A relevant aspect of our analysis is that we did not remove a trend from the data before calculating the EOFs and PCs. This is consistent with the original calculations of EOFs in the North Pacific (Davis, 1976) and more recent analysis by Johnstone and Mantua (2014), but inconsistent with the definition of the PDO which did have a global mean trend removed (Mantua et al., 1997; Zhang et al., 1997). Whether or not a trend was removed had little effect on the first EOF, and thus the PDO, until 2014. Two of our results lead to this conclusion: first, our first PC calculated between 1950 and 1993 agreed with the PDO with a correlation coefficient of 0.97; and second, our first EOF calculated with successively longer time series did not change in shape until 2014. There are many approaches to removing a trend from time series (Deser & Phillips, 2021; Frankignoul et al., 2017; Solomon & Newman, 2012). We investigated two of these approaches: first we removed a least-squares fit of a line to the global average temperature as in the original definition of the PDO (Figure S2 in Supporting Information S1), and second, we removed a least-squares fit of a line from each grid point in the North Pacific (Figure S3 in Supporting Information S1). In each case the EOF analysis reproduced the PDO spatial pattern and index, suggesting that the PDO remains a good measure for the variability relative to the trend. In general, removal of a trend (as by least-squares fitting of a line, e.g.) tends to deemphasize the ends of a record. In our analysis, the inclusion of the trend highlights the fact that the warming in the eastern Pacific has increased notably in recent years, a fact that would be obscured if a linear trend had been removed.

The PDO is recognized to be a result of many processes that may cause temperature variability (Newman et al., 2016) rather than any singular phenomenon. The many processes that affect SST have apparently combined to create both this era of frequent marine heatwaves beginning in 2014 and a fundamental change to the first mode of SST. The persistence of the marine heatwaves was studied by Di Lorenzo and Mantua (2016) who also invoked a number of interacting processes, suggesting that the variance described by the PDO would increase in a warmer climate. Di Lorenzo and Mantua (2016) explicitly removed a trend before calculating the EOFs of SST, so that their EOFs described variance relative to the trend. The PDO is based on a constant spatial pattern defined by the EOF that described the most variance of SST through the mid 1990's. However, there is no guarantee that the EOFs of SST will remain constant as climate change continues. This concern about indices based on EOFs applies also to the North Pacific Gyre Oscillation (Di Lorenzo et al., 2008), which describes variance in sea surface height.

The PDO is widely used as a measure of temperature in the eastern boundary upwelling system along the west coast of North America (e.g., Weber et al., 2021). The period of persistent marine heatwaves since 2014 has made the PDO less useful as an index of temperature in this region because it does not reflect the recent increase. In general, using PCs from a basin-wide analysis as indices of temperature for specific regions may be problematic because the influences from distant parts of the basin affect the PCs. Options moving forward may include: (a) updating the definition of the first mode of temperature variability, as we have done here, (b) explicitly accounting for the trend in addition to the PDO for a measure of temperature, or (c) defining a new temperature metric in a specified area in the region as is done for the various measures of El Niño (Trenberth, 1997) or more recently as in the NEP index (Johnstone & Mantua, 2014). Interestingly, the NEP was first published just before the recent period of MHWs, and the value of the approach championed in Johnstone and Mantua (2014) has only increased. The wide-ranging effects of the recent period of MHWs are likely to be seen in continuing studies of the eastern North Pacific.

Data Availability Statement

We use monthly mean SST for the period 1950–2021 in the region 120°E–110°W, 20°N–60°N, from the NOAA Extended Reconstructed Sea Surface Temperature V5 data set (Huang et al., 2017a), retrieved from <https://psl.noaa.gov/data/gridded/data.noaa.ersst.v5.html> on 12 January 2022. The Pacific Decadal Oscillation Index was downloaded from <https://www.ncei.noaa.gov/access/monitoring/pdo/> on 21 October 2022.

Acknowledgments

The authors gratefully acknowledge the support of the National Oceanic and Atmospheric Administration through the Global Ocean Monitoring and Observing program (NA20OAR4320278) and the Southern California Coastal Ocean Observing System (NA21NOS0120088). The authors thank Nate Mantua and an anonymous reviewer for helpful comments.

References

- Amaya, D. J., Miller, A. J., Xie, S. P., & Kosaka, Y. (2020). Physical drivers of the summer 2019 North Pacific marine heatwave. *Nature Communications*, 11(1), 1903. <https://doi.org/10.1038/s41467-020-15820-w>
- Bond, N. A., Cronin, M. F., Freeland, H., & Mantua, N. (2015). Causes and impacts of the 2014 warm anomaly in the NE Pacific. *Geophysical Research Letters*, 42(9), 3414–3420. <https://doi.org/10.1002/2015gl063306>
- Bond, N. A., Overland, J. E., Spillane, M., & Stabeno, P. (2003). Recent shifts in the state of the North Pacific. *Geophysical Research Letters*, 30(23), 2183. <https://doi.org/10.1029/2003gl018597>
- Davis, R. E. (1976). Predictability of sea surface temperature and sea level pressure anomalies over the North Pacific Ocean. *Journal of Physical Oceanography*, 6(3), 249–266. [https://doi.org/10.1175/1520-0485\(1976\)006<0249:possta>2.0.co;2](https://doi.org/10.1175/1520-0485(1976)006<0249:possta>2.0.co;2)
- Deser, C., & Phillips, A. S. (2021). Defining the internal component of Atlantic multidecadal variability in a changing climate. *Geophysical Research Letters*, 48(22), e2021GL095023. <https://doi.org/10.1029/2021GL095023>
- Di Lorenzo, E., & Mantua, N. (2016). Multi-year persistence of the 2014/15 North Pacific marine heatwave. *Nature Climate Change*, 6(11), 1042–1047. <https://doi.org/10.1038/nclimate3082>
- Di Lorenzo, E., Schneider, N., Cobb, K. M., Franks, P. J. S., Chhak, K., Miller, A. J., et al. (2008). North Pacific Gyre Oscillation links ocean climate and ecosystem change. *Geophysical Research Letters*, 35(8), L08607. <https://doi.org/10.1029/2007gl032838>
- Frankignoul, C., Gastineau, G., & Kwon, Y. O. (2017). Estimation of the SST response to anthropogenic and external forcing and its impact on the Atlantic multidecadal oscillation and the Pacific decadal oscillation. *Journal of Climate*, 30(24), 9871–9895. <https://doi.org/10.1175/Jcli-D-17-0009.1>
- Huang, B., Thorne, P. W., Banzon, V. F., Boyer, T., Chepurin, G., Lawrimore, J., et al. (2017a). *NOAA extended reconstructed sea surface temperature (ERSST), Version 5*. NOAA National Centers for Environmental Information. <https://doi.org/10.7289/V5T72FNM>
- Huang, B. Y., Thorne, P. W., Banzon, V. F., Boyer, T., Chepurin, G., Lawrimore, J. H., et al. (2017b). Extended reconstructed sea surface temperature, Version 5 (ERSSTv5): Upgrades, validations, and intercomparisons. *Journal of Climate*, 30(20), 8179–8205. <https://doi.org/10.1175/Jcli-D-16-0836.1>
- Johnstone, J. A., & Mantua, N. J. (2014). Atmospheric controls on northeast Pacific temperature variability and change, 1900–2012. *Proceedings of the National Academy of Sciences of the United States of America*, 111(40), 14360–14365. <https://doi.org/10.1073/pnas.1318371111>
- L'Heureux, M. L., Takahashi, K., Watkins, A. B., Barnston, A. G., Becker, E. J., Di Liberto, T. E., et al. (2017). Observing and predicting the 2015/16 El Niño. *Bulletin of the American Meteorological Society*, 98(7), 1363–1382. <https://doi.org/10.1175/Bams-D-16-0009.1>

- Litzow, M. A., Hunsicker, M. E., Bond, N. A., Burke, B. J., Cunningham, C. J., Gosselin, J. L., et al. (2020). The changing physical and ecological meanings of North Pacific Ocean climate indices. *Proceedings of the National Academy of Sciences of the United States of America*, 117(14), 7665–7671. <https://doi.org/10.1073/pnas.1921266117>
- Litzow, M. A., Malick, M. J., Bond, N. A., Cunningham, C. J., Gosselin, J. L., & Ward, E. J. (2020). Quantifying a novel climate through changes in PDO-Climate and PDO-salmon relationships. *Geophysical Research Letters*, 47(16), e2020GL087972. <https://doi.org/10.1029/2020GL087972>
- Mantua, N. J., Hare, S. R., Zhang, Y., Wallace, J. M., & Francis, R. C. (1997). A Pacific interdecadal climate oscillation with impacts on salmon production. *Bulletin of the American Meteorological Society*, 78(6), 1069–1079. [https://doi.org/10.1175/1520-0477\(1997\)078<1069:Apicow>2.0.Co;2](https://doi.org/10.1175/1520-0477(1997)078<1069:Apicow>2.0.Co;2)
- Namias, J., & Cayan, D. R. (1981). Large-scale air-sea interactions and short-period climatic fluctuations. *Science*, 214(4523), 869–876. <https://doi.org/10.1126/science.214.4523.869>
- Newman, M., Alexander, M. A., Ault, T. R., Cobb, K. M., Deser, C., Di Lorenzo, E., et al. (2016). The Pacific decadal oscillation, revisited. *Journal of Climate*, 29(12), 4399–4427. <https://doi.org/10.1175/Jcli-D-15-0508.1>
- Newman, M., Compo, G. P., & Alexander, M. A. (2003). ENSO-forced variability of the Pacific decadal oscillation. *Journal of Climate*, 16(23), 3853–3857. [https://doi.org/10.1175/1520-0442\(2003\)016<3853:Evotpd>2.0.Co;2](https://doi.org/10.1175/1520-0442(2003)016<3853:Evotpd>2.0.Co;2)
- Ren, A. S., & Rudnick, D. L. (2021). Temperature and salinity extremes from 2014–2019 in the California Current System and its source waters. *Communications Earth & Environment*, 2(1), 62. <https://doi.org/10.1038/s43247-021-00131-9>
- Rudnick, D. L., Zaba, K. D., Todd, R. E., & Davis, R. E. (2017). A climatology of the California Current System from a network of underwater gliders. *Progress in Oceanography*, 154, 64–106. <https://doi.org/10.1016/j.pocan.2017.03.002>
- Solomon, A., & Newman, M. (2012). Reconciling disparate twentieth-century Indo-Pacific Ocean temperature trends in the instrumental record. *Nature Climate Change*, 2(9), 691–699. <https://doi.org/10.1038/Nclimate1591>
- Trenberth, K. E. (1997). The definition of El Niño. *Bulletin of the American Meteorological Society*, 78(12), 2771–2777. [https://doi.org/10.1175/1520-0477\(1997\)078<2771:Tdoeno>2.0.Co;2](https://doi.org/10.1175/1520-0477(1997)078<2771:Tdoeno>2.0.Co;2)
- Weare, B. C., Navato, A. R., & Newell, R. E. (1976). Empirical orthogonal analysis of Pacific sea-surface temperatures. *Journal of Physical Oceanography*, 6(5), 671–678. [https://doi.org/10.1175/1520-0485\(1976\)006<0671:Eoaoops>2.0.Co;2](https://doi.org/10.1175/1520-0485(1976)006<0671:Eoaoops>2.0.Co;2)
- Weber, E. D., Auth, T. D., Baumann-Pickering, S., Baumgartner, T. R., Bjorkstedt, E. P., Bograd, S. J., et al. (2021). State of the California current 2019–2020: Back to the future with marine heatwaves? *Frontiers in Marine Science*, 8(1081). <https://doi.org/10.3389/fmars.2021.709454>
- Wen, C. H., Kumar, A., & Xue, Y. (2014). Factors contributing to uncertainty in Pacific Decadal Oscillation index. *Geophysical Research Letters*, 41(22), 7980–7986. <https://doi.org/10.1002/2014gl061992>
- Zaba, K. D., & Rudnick, D. L. (2016). The 2014–2015 warming anomaly in the Southern California Current System observed by underwater gliders. *Geophysical Research Letters*, 43(3), 1241–1248. <https://doi.org/10.1002/2015GL067550>
- Zhang, Y., Wallace, J. M., & Battisti, D. S. (1997). ENSO-Like interdecadal variability: 1900–93. *Journal of Climate*, 10(5), 1004–1020. [https://doi.org/10.1175/1520-0442\(1997\)010<1004:eliv>2.0.co;2](https://doi.org/10.1175/1520-0442(1997)010<1004:eliv>2.0.co;2)
- References From the Supporting Information
- Deser, C., Simpson, I. R., McKinnon, K. A., & Phillips, A. S. (2017). The northern hemisphere extratropical atmospheric circulation response to ENSO: How well do we know it and how do we evaluate models accordingly? *Journal of Climate*, 30(13), 5059–5082. <https://doi.org/10.1175/Jcli-D-16-0844.1>
- Deser, C., Simpson, I. R., Phillips, A. S., & McKinnon, K. A. (2018). How well do we know ENSO's climate impacts over North America, and how do we evaluate models accordingly? *Journal of Climate*, 31(13), 4991–5014. <https://doi.org/10.1175/Jcli-D-17-0783.1>
- Rayner, N. A., Parker, D. E., Horton, E. B., Folland, C. K., Alexander, L. V., Rowell, D. P., & Kaplan, A. (2003). Global analyses of sea surface temperature, sea ice, and night marine air temperature since the late nineteenth century. *Journal of Geophysical Research*, 108(D14), 4407. <https://doi.org/10.1029/2002jd002670>